Study on Clouds and Marine Atmospheric Boundary Layer

Zhao Bolin (赵柏林), *Zhen Jinming* (甄进明), *Hu Chengda* (胡成达), *Du Jinlin* (杜金林), *Zhu Yuanjing* (朱元竞) and *Zhang Chengxiang* (张呈祥)
Department of Geophysics, Peking University, Beijing 100871
Received January 14, 1992; revised April 23, 1992

ABSTRACT

A set of remote sensing instruments of Peking University, which includes mainly a dual-channel(22.235GHz and 35.5GHz) microwave radiometer, a 8mm microwave and a 5mm microwave radiometer, has been developed for the Western North-Pacific Cloud-Radiation Experiment (WENPEX). The instruments were used to observe the cloud and marine atmospheric boundary-layer in the southwest sea area of Japan in winter time from 1989 to 1991.In the weather change process, the characteristics of the marine atmospheric boundary-layer and liquid water content in cloud of this area in winter time are studied from observation data. A one-dimensional mixed layer model is presented for the growth and evolution of a cloud-topped marine boundary-layer. The model is used to study in the WENPEX. The simulation results are in agreement with observation data, especially the integral water in cloud.

I. INTRODUCTION

The Western North-Pacific Cloud-Radiation Experiment (WENPEX), which was a regional experiment of the International Satellite Cloud Climatology Project (ISCCP). It was designed to investigate the physical mechanism of climate change, the influence of cloud and radiation on climate change. WENPEX was mainly conducted by Japanese scientists, under the leadership of Prof. Takao Takeda. Peking University was invited to take part in this experiment and used a set of remote sensing instruments to observe the cloud and marine atmospheric boundary-layer. The analysis and parameterization of these processes are very important in the research of climate change.

WENPEX was conducted in winter time from 1989 to 1991. The pilot experiment was carried on in February of 1989 in Shionomisaki of Japan. The main experiment was in January of 1990 and January of 1991 in Amami Oshima of Japan. There were satellite observation, aeroplane observation, ship observation, and ground-based island observation.

In this paper, the results and analysis of Peking University's ground-based island observation are presented.

II. OBSERVATION INSTRUMENTS

The instruments, Peking University brought to WENPEX are mainly a set of microwave radiometers made by Peking University. They are as follows:

dual-channel(22.235GHz and 35.3GHz) microwave radiometer;

8 mm (35.3Ghz) microwave radiometer; 5 mm (54.5GHz) microwave radiometer;

infrared radiometer (window channel 8-13 μm), barometer, dry and wet bulb hygrometer, etc.

The observation items are total atmospheric vapor, atmospheric vapor profile, integral liquid water in cloud, distribution of cloud liquid water in whole sky, cloud base height, relative rain intensity and low level temperature profile, etc.

(1) The dual-channel (22.235GHz and 35.3GHz) microwave radiometer is shown in Fig.1. The radiometer has an antenna for 8 mm-1.35 cm wave band. Signals enter a circular wave guide feed and are separated by waveguide polarization with different frequencies, then go into 8 mm and 1.35 cm receivers independently. There are two reference loads with temperature of 313K and 413K. They are put into each receiver, and used to calibrate the receiver's gain. Signals pass through mixer and amplifers and then output to an Apple-II computer for sampling and data processing. With antenna zenith observation, the profile of atmospheric vapor content may be derived. Microwave radiometer observations can be carried on with elevation and azimuthal angle scanning, then the distribution of cloud water content of whole sky is obtained. The data processing and radiometer observations are automatically conducted by use of the Apple-II microcomputer. Microcomputer is used to control the scanning and sampling. Both elevation scanning observation (in θ direction) and azimuth scanning observation (in φ direction) are available. From the received information of the two frequencies, the total atmospheric vapor and the integral liquid water content in cloud can be deduced (Zhao 1989, 1990).

(2) 5mm microwave radiometer is Dicke's type radiometer. It is controlled and takes samples by Apple-II computer, as shown in Fig.1. A set of brightness temperatures can be gained by elevation angle scanning observation. The temperature profile from surface to 700hPa can be retrieved from the brightness temperatures (Zhao et al., 1991).

(3) 8mm microwave radiometer is Dicke's type radiometer also, and takes samples by Apple-II computer. This radiometer is designed to set under caves and to observe at 45° elevation angle, so that the cloud and rain in all weather can be observed (see Fig.1). Its brightness temperature varied with the integral liquid water in cloud and rain intensity.

III. OBSERVATION AND WEATHER CONDITION

The ground-based island observation of WENPEX was at Arkasaki (28° 24′N, 129° 29′E), Amami Oshima, Japan. Two periods of observation were from Jan. 10 to Jan. 26 in 1990 and from Jan. 9 to Jan. 28 in 1991. It is common that there are clouds in sky, which are cumulus, stratocumulus, and nimbus-status with weather changing.

Cloud and werther processes are closely related. In winter, the weather process of Amami Oshima can be characterized by that it is controlled in turn by dry cold air from Northwest China continent and wet warm air from South China Sea aera. The variations of surface pressure, temperature, sea surface temperature and total atmospheric vapor are shown in Fig.2. The dry cold air is accompanied with high pressure, low temperature and small atmospheric vapor, and the wet warm air is accompanied with low pressure, high temperature and large total atmospheric vapor. These two kinds of air take place alternatively and the cyclicity is about four days. Although the surface temperature variation is very large (± 6.0K), the sea surface temperature only changes a little (± 1.6K). Except under strong south wind, the sea surface temperature is keeping higher than surface temperature.

IV. CHARACTERISTICS OF CLOUD AND MARINE ATMOSPHERIC BOUNDARY LAYER

In witer, the change of weather process in Amami Oshima, Japan, is in a cyclical way. This cyclicity makes the marine atmospheric boundary layer also change periodically. In Fig.3, from radiosonde data, the variation of temperature and humidity profiles from Jan. 16

to Jan. 17 of 1991 are given. Fig.3(a) is at 08 hour of Jan. 16. At that moment Amami Oshima was controlled by dry cold air. When the dry cold air from Northwest China continent came to the warm sea water, the heating in low part of air due to the warm surface sea water led to unstability. So that the turbulence was active and convective boundary-layer, mixed layer formed. As shown in Fig.3(a), the potential temperature and mixing ratio are constant with height, indicating that the layer is well mixed. At the top of the mixed layer, there were discontinuities in temperature and humidity, a strong inversion and a sharp decrease in mixing ratio. Because of the warm sea surface water, the mixed layer gained heat and humidity flux from sea surface. Fig.3(b) is at 20 hour of Jan. 16. At that moment the surface pressure decreased, surface temperature increased, total atmospheric vapor increased. There was a region at about 700 hPa where the relative humidity was large, that attributes to the wet warm air intruded and climbed on the dry cold air. The inversion at about 800 hPa was nearly to disappear. Fig.3(c) is at 08 hour of Jan. 17. At that moment the surface pressure lowered further, surface temperature further increased, total atmospheric vapor increased more and some rain came. Amami Oshima was controlled by wet warm air. Fig.3(d) is at 20 hour of Jan. 17. At that moment the surface pressure returned to high, surface temperature decreased back, total atmospheric vapor lowered. Amami Oshima was controlled by dry cold air again. The mixed layer came back, the temperature and humidity profiles were similar to that in Fig.3(a).

The periodic variation of the marine atmospheric boundary layer determines the characteristics of cloud in this area. Cold and warm front cloud systems are due to dry cold air and wet warm air taking place in turn. The cold front can develop to the height about 500 hPa, the integral liquid water in cloud is large and often accompanied with rain. Another kind of cloud is the low level cumulus and stratocumulus in the marine atmospheric boundary layer. It is due to the fact that the dry cold air comes to warm sea water, thus a mixed layer forms, water vapor is constantly transferred from sea surface into the mixed layer. So that condensation takes place in upper part of the mixed layer and cloud forms.

Some characteristics of the integral liquid water in cloud are concluded from the observation results in Amami Oshima, Japan, in January of 1990 and 1991.

1. The low level cumulus and stratocumulus in the marine atmospheric boundary-layer occur very frequently. The integral liquid water in cloud is about 0.1mm, seldom more than 0.3mm. And generally the integral liquid water in cumulus is less than in stratocumulus. In Fig.4, the continuous observation result of dual-channel microwave radiometer at zenith from 13:30 Jan. 20 to 13:30 Jan. 21 in 1990 is given. As shown in Fig.4, the integral liquid water in cloud is below 0.3mm. In Fig.5, the whole-sky scanning (θ: 30°–90° , φ: 0° –360°) observation result of dual-channel microwave radiometer in cloud in whole sky can be seen in this figure, and maximum is 0.25mm.

2. The integral liquid water changes obviously when rain comes. The cumulus and stratocumulus in marine atmospheric boundary-layer rarely cause rain. For a few cases that the convective cloud is very active, there is a very-short-time shower. In Fig.6, the observation result of continuous azimuth scanning at an elevation angle of 45° from 17:13 to 20:18 on Jan. 13, 1991 is given. As shown in the figure, the integral liquid water in cloud varied under 0.2 mm. Beginning from 19:35, there was a region where the integral liquid water in cloud surpassed 0.3 mm and the microwave Doppler-radar of Nagoya University detected a small shower, it lasted only 6 minutes.

There is a rapid increasing in integral liquid water in cloud, surpassing 0.5 mm, and then

the rain of the cloud system came. In Fig.7, the continuous observation result of microwave radiometer at zenith on Jan. 18, 1990 is shown. There was a rapid increasing in the integral liquid water included at 12:10, and the frontal rain cloud system came and rain took place. The variation of the total atmospheric vapor and integral water in cloud from 15:00–20:30 on Jan. 17, 1991 are shown in Fig.8. There was a continuous rain in the morning of Jan. 17 due to the wet warm air intruded. In the afternoon, dry cold air came, the total atmospheric vapor and the integral liquid water in cloud were in decreasing.

3. 8 mm microwave radiometer was set under caves and the antenna directed at 45° elevation angle. So that it can observe continuously when it rains. The variation of observed brightness temperature of this microwave radiometer from 09:00 to 20:00 on Jan. 25, 1991 is shown in Fig.9. There were some rains in this observation period and brightness temperature gave change with rain. That is, when there was rain, the brightness temperature was at a greater value. This result agrees with the microwave Doppler–radar observation result.

4. 5 mm microwave radiometer remotely senses the temperature profile from surface to 700 hPa by elevation angle scanning observation. The continuous variations of temperature profile can be gained by every 3 hours microwave radiometer observation. The variation of temperature profile retrieved from the radiometer observation from 8:30 to 20:30 on Jan. 16, 1991 is shown in Fig.10.

V. MODEL STUDY OF CLOUD-TOPPED MARINE ATMOSPHERIC BOUNDARY LAYER

A one-dimensional mixed layer model is presented for growth and evolution of a cloud-topped marine boundary layer. In this model, the entrainment rate is determined from the turbulence kinetic energy budget. The mixed layer depth or cloud top height, the condensation level or cloud base height, the integral liquid water in cloud are main subjects to be simulated. The parameterization adopted in the present model is used in the mixed layer model of Lilly (1968). The entrainment rate in a cloud -topped atmospheric boundary layer developed by Stage and Businger (1981), is adopted. The model is designed to simulate the convective atmospheric boundary layer, which occurs when dry cold air comes over warm water. The cumulus and stratocumulus developing and maintaining can be simulated. (see Fig.11).

Horizontal homogeneity is assumed, so advection terms are neglected. The governing equations are

$$\frac{\partial \theta_1}{\partial t} = \frac{(\overline{W'\theta'_1}|_0 - \overline{W'\theta'_1}|_i - R_c - R_b)}{Z_i}, \tag{1}$$

$$\frac{\partial q_t}{\partial t} = \frac{(\overline{W'q'}|_0 - \overline{W'q'}|_i)}{Z_i}, \tag{2}$$

$$\frac{\partial Z_i}{\partial t} = W_e + W_d, \tag{3}$$

where $\theta_1 = \theta_e - \frac{l}{C_p} q_l$, θ_1 is liquid water potential temperature, L the latent heat of evaporization, C_p the specific heat at constant pressure, and q_1 liquid water mixing ratio.

$$q_t = \begin{cases} q_s + q_l & \text{when saturated} \\ q & \text{when unsaturated} \end{cases} \tag{4}$$

θ_l and q_t are conservative equation, and assumed to be same within the mixed layer, $\overline{W'\theta'_l}\big|_t$ and $\overline{W'q'_t}\big|_t$ are turbulent fluxes at the top of mixing layer.

$$\overline{W'\theta'_l}\big|_t = -W_e\Delta\theta_l,$$

$$\overline{W'q'_t}\big|_t = -W_e\Delta q_t, \tag{5}$$

$\Delta\theta_l$ and Δq_t are mean jumps of θ_l and q_t across the mixed layer top. $\overline{W'\theta'_l}\big|_o$ and $\overline{W'q'_t}\big|_0$ are surface turbulent flux, i.e.,

$$\overline{W'\theta'_l}\big|_0 = C_h U\ (\theta_0 - \theta_l)\ ,$$

$$\overline{W'q'_t}\big|_0 = C_q U\ (q_{t0} - q_t)\ , \tag{6}$$

C_q and C_h are transfer coefficients of moisture and heat, U is the wind speed at 10 m above sea level, θ_0 is the sea surface temperature, q_{to} the saturated mixing ratio at this temperature. R_b is the infrared cooling rate near the cloud top and R_c the infrared radiation warming rate near the cloud base, i.e.,

$$R_b = \frac{\sigma}{\rho C_p}(T_b^4 - T_s^4),$$

$$R_c = \frac{\sigma}{\rho C_p}(T_o^4 - T_c^4), \tag{7}$$

σ is Stefan–Boltzmann constant, ρ is the air density, T_s is the radiative sky temperature, T, T_c and T_0 are temperatures at cloud top, cloud base and sea surface, respectively. When no clouds are present, R_b and R_c are set to zero. The solar radiation, has been neglected in presented model. W_d is lifting rate of mixed layer top due to large-scale convergence.

$$W_d = -Z_i\nabla_h \cdot V, \tag{8}$$

Z_i is the depth of the mixed layer. $\nabla_h \cdot V$ is divergence. According to Stage and Businger (1981), the dissipation rate is a fixed fraction $(1-A)$ of the production rate and the buoyant production P and consumption N of kinetic energy can be written as

$$P = gT^{-1}\int_0^{Z_i}\overline{W'\theta'_v}\big|_{\text{production}}dZ = \frac{1}{2}gt^{-1}Z_i\ (P_1 + P_2 + W_e P_3)\ ,$$

$$N = gT^{-1}\int_0^{Z_i}\overline{W'\theta'_v}\big|_{\text{consumption}}dZ = \frac{1}{2}gt^{-1}Z_i\ (N_1 + N_2 + W_e N_3)\ , \tag{9}$$

and

$$N = A \cdot P, \tag{10}$$

$$W_e = \frac{A(P_1 + P_2) - (N_1 + N_2)}{N_3 - AP_3}, \tag{11}$$

for no cloud

$$W_e = \frac{A\ \overline{W'\theta'_v}\big|_0}{\Delta\theta_v}, \tag{12}$$

the production and consumption terms can be divided into non-entrainment (P_1 ,N_1), radiation (P_2 ,N_2), and entrainment (W_e P_3 ,W_e N_3). θ_v is the virtual potential temperature. Δ denotes mean jumps across the inversion base (upper minus lower). See Stage and Businger (1981).

Simulation study of WENPEX:

The initial condition is based on the Amami Oshima radiosonde data, and sea surface temperature is taken as 18℃, sea surface wind speed 7 ms^{-1} , and large-scale lifting rate is set to zero. The simulated evolution of the mixed layer of this case is shown in Fig.12. Because of the constant sea surface turbulent transfer to the mixed layer and entrainment from above air, the mixed layer depth deepens at a small speed, as shown in Fig.12. Within 7 hrs, the increase of the mixed layer depth is about 200 m. And the lifting condensation level gets lower and lower due to the changes of the heat and moisture in the layer. In this case the cloud top gets higher while cloud base gets lower, that makes the cloud layer develop and thicken. As shown in Fig.12, the integral water in cloud increases from 0.039 mm to 0.371 mm.

The large-scale lifting rate W_d is very significant in the evolution of the mixed layer. Unlike the entrainment rate which only makes the mixed layer deepen by entraining air from above, the large-scale lifting rate W_d can be postive in convergence and negative in divergence, so that it may deepen or shrink the mixed layer. Especially, when the mixed layer is fully developed, the entrainment rate is small, so the large-scale lifting rate plays a key role in the mixed layer evolution.

In the convergence area, W_d is positive. The mixed layer develop faster and cloud layer grows thicker. The integral liquid water in cloud also increases fast, and there will be rain. As shown in Fig.13, the same conditions are taken as in Fig.12, but the large-scale lifting rate is set to 0.01 ms^{-1} . Compared with Fig.12 the mixed layer grows faster, and integral liquid water in cloud grows from 0.039 mm to over 0.500 mm. According to observations of the integral liquid water in cloud by microwave radiometer, when the integral liquid water in cloud becomes more than 0.30 mm, rain may come. The large-scale convergence makes the cloud develop and breaks the limit of atmospheric boundary layer, no further simulation is conducted by the present model.

In the divergence area, W_d is negative. The mixed layer is determined by both W_e and W_d. On Jan.18, 1991, Amami Oshima was under a high pressure, there was a divergence. From the radiosonde data of 08:30 and 20:30 on Jan.18, the mixed layer became thinner. And in this period, the stratocumulus transited to cumulus, and then disappeared.

The initial condition is based on the 06:30 Jan.18 radiosonde data, $\nabla_h V$ is set to 0.000015 $s^{-1}$and 0.000025 s^{-1}. Simulation results are shown in Fig.14 and Fig.15. W_d is gotten from Eq.(8). In Fig.14, the W_d is only a little greater than entrainment rate W_e, the mixed layer depth gets thinner very slowly, also the integral liquid water in cloud decreases very slowly. In Fig.15, the W_d is much larger than W_e , the mixed layer becomes thinner faster than that in Fig.14, and integral liquid water in cloud decreases to zero. The simulated evolution of the mixed layer in Fig.15 is more agreeable with the real circumstance in WENPEX.

The authors wish to express their thanks to Prof. Takao Takeda for having invited Peking University group to

take part in WEXPEX and having provided financial support when they stayed in Japan. In China this work is supported by National Natural Science Foundation of China (NNSFC).

REFERENCES

Lilly D.K. (1968), Models of cloud topped mixed layer under a strong inversion, *Q. J. Roy. Meteorol. Soc.*, **94**: 292.

Stage S.A. and J.A. Businger (1981), A model for entrainment into a cloud topped marine boundary layer, *J. Atmos.Sci.* **38**: 2213–2229.

Zhao Bolin (1989), Study on cloud and rain by microwave radiometer observation, *Atmospheric Research*, **24(4)**: 33–43.

Zhao Bolin (1990), Study on microwave remote sensing of atmosphere, cloud and rain, *Advances in Atmos. Sci.*, **7**: 475–430.

Zhao Bolin, Fu Qiang, Hu Chengda and Li Huixin (1991), Study on microwave remote sensing of atmospheric properties and weather process, *Science in China*, *34B*: 352–362.

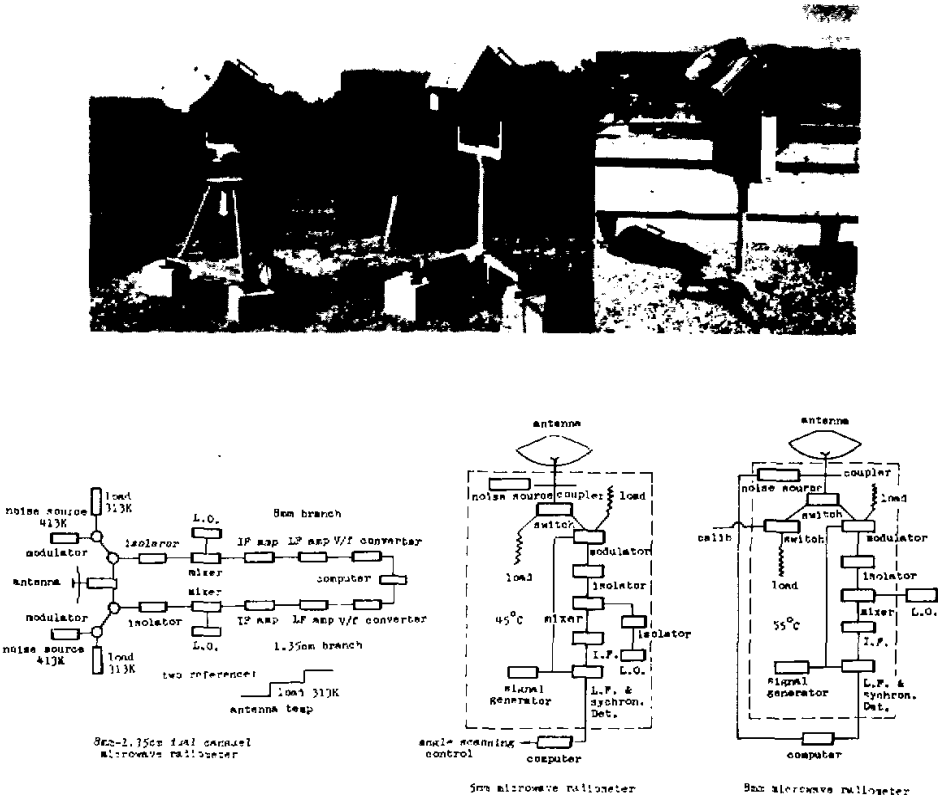

Fig.1. Multifrequency microwave radiometer (a) and their schematic diagrams (b); 8 mm–1.35 cm dual channel microwave radiometer(left, 8 mm, 35.3 GHz, and 1.35 cm, 22.235 GHz), 5 mm microwave radiometer(middle, 5 mm, 54.5 GHz),and 8mm microwave radiometer (right, 8 mm, 35.3 GHz).

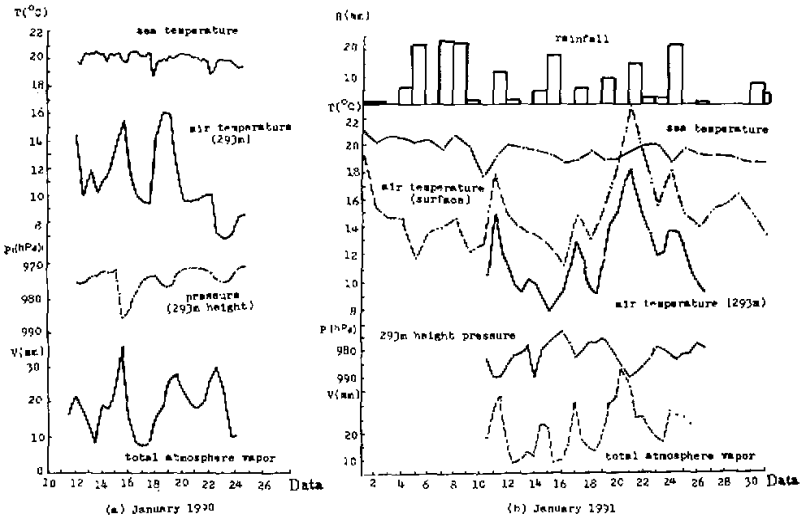

Fig.2. The variation of meteorological elements of marine atmosphere. (a) January 1990 (b) January 1991.

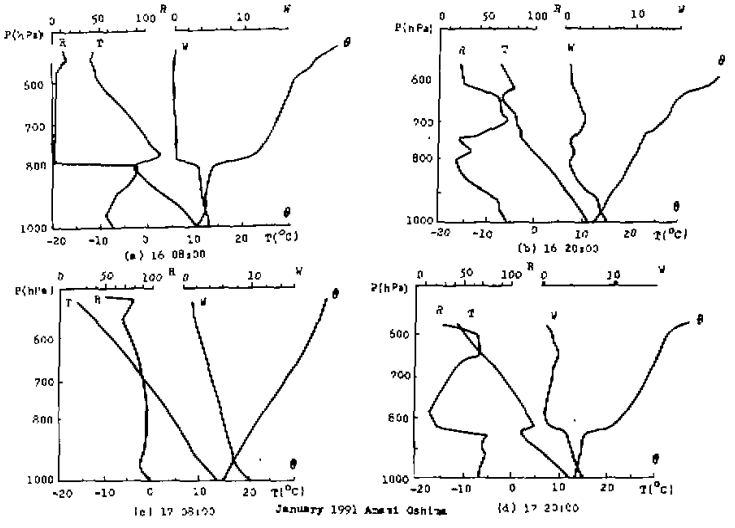

Fig.3. The weather process and the structure of marine atmosphere. (a) 16 08:00 (b) 16 20:00 (c) 17 08:00 (d) 17 20:00.

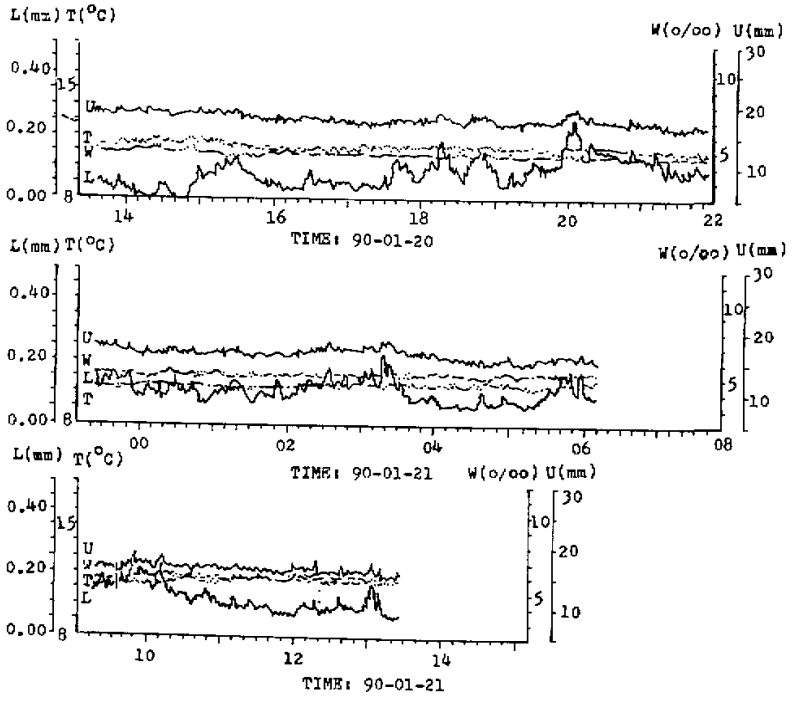

Fig.4. The diurnal variation of liquid water content of cloud L, the total water content U, the surface temperature T and the surface mixing ratio W. R: relative humidity, T: temperature, θ: potential temperature, W: mixing ratio.

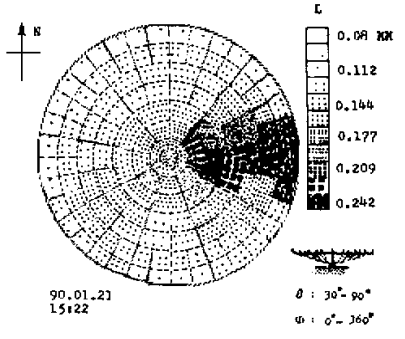

Fig.5. Distribution of liquid water content of cloud in the whole sky.

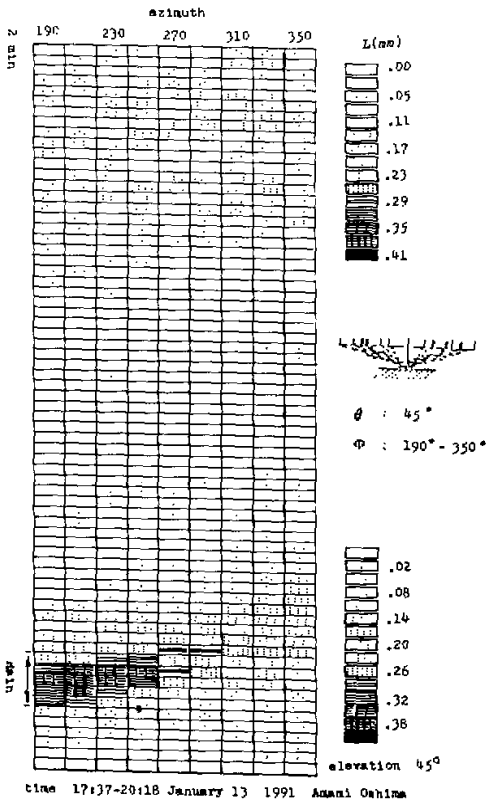

Fig.6. Cloud liquid content distribution in sky and its variation.

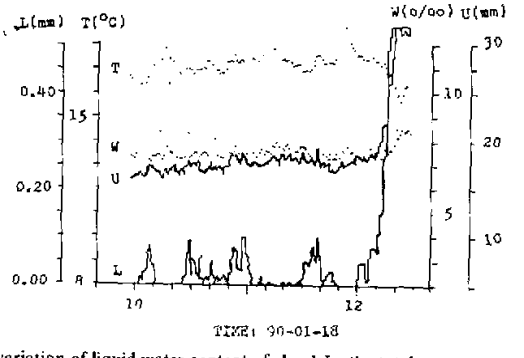

Fig.7. The variation of liquid water content of cloud L, the total water vapor content U, the surface mixing ratio W and surface temperature T (before rain).

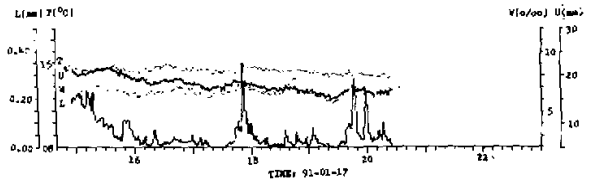

Fig.8. As in Fig.7. but after rain.

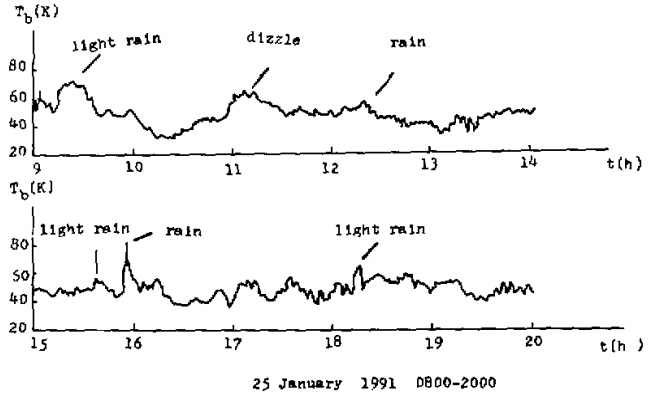

Fig.9. Variation of 8 mm brightness temperature at elevation angle 45°.

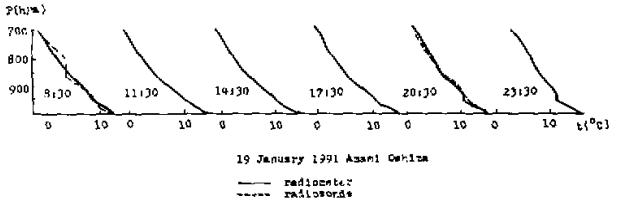

Fig.10. Diurnal variation of atmospheric temperature profile observed by 5 mm microwave radiometer in comparison with that of radiosonde observation.

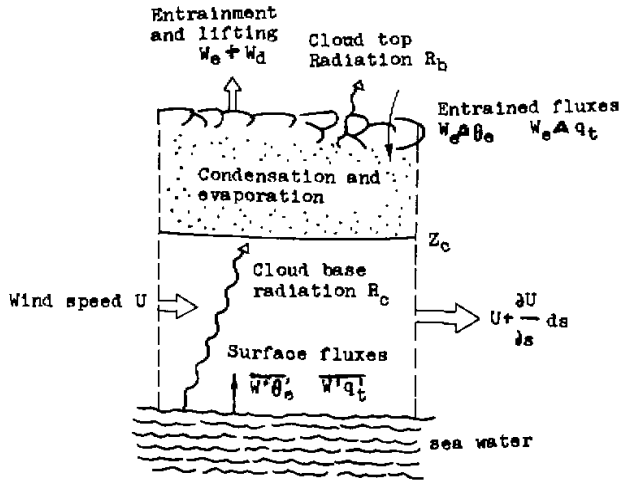

Fig.11. Schematic diagram of process acting on a cloud-topped marine boundary (Stage and Businger, 1981).

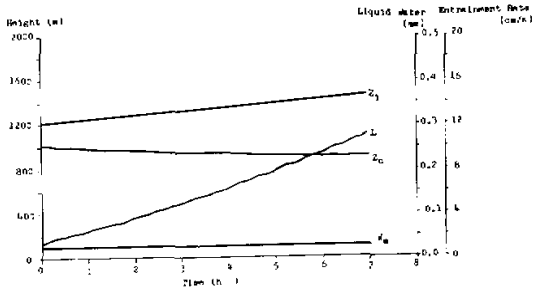

Fig.12. The evolution of the boundary layer(Z_1: depth of the mixed layer, Z_c: condensatinon level, L: integral liquid water in cloud, W_e: entrainment rate) lifting rate = 0.00.

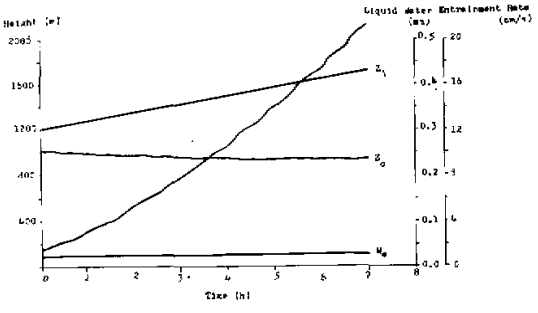

Fig.13. As in Fig. 12, but for lifting rate = 0.01 ms $^{-1}$.

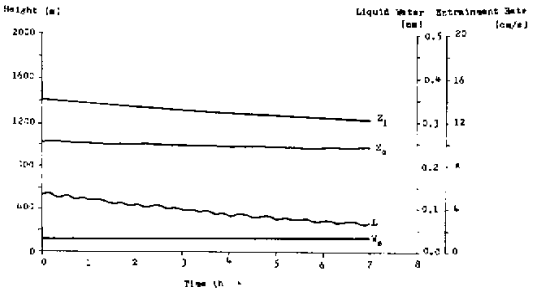

Fig.14. The evolution of boundary layer (Z_i: depth of mixed layer, Z_c: condensation level. L: integral liquid water in cloud, W_e: entrainment rate) divergence = 0.000015 s^{-1}.

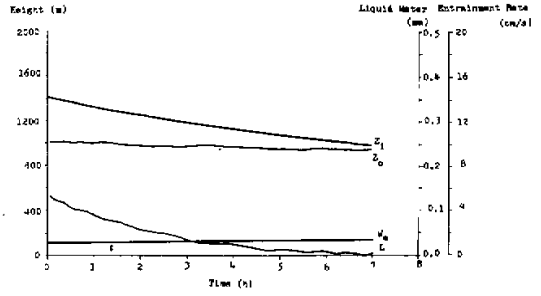

Fig.15. As in Fig.14, but for divergence = 0.000025 s^{-1}.